The developing T-cell compartment of the neonatal lung orchestrates an atypical response to respiratory syncytial virus

Thomas Démoulins[1,2], Melanie Brügger[1,2,3], Beatrice Zumkehr[1,2], Blandina I. Oliveira Esteves[1,2], Kemal Mehinagic[1,2,3,4], Amal Fahmi[1,2,3], Loïc Borcard[1,2,3], Horst Posthaus[4,5], Charaf Benarafa[1,2], Nicolas Ruggli[1,2], and Marco P. Alves[1,2,*]

[1] *The Institute of Virology and Immunology, Mittelhäusern and Bern, Switzerland*

[2] *Department of Infectious Diseases and Pathobiology, Vetsuisse Faculty, University of Bern, Bern, Switzerland*

[3] *Graduate School for Cellular and Biomedical Sciences, University of Bern, Bern, Switzerland*

[4] *Institute of Animal Pathology, Department of Infectious Diseases and Pathobiology, Vetsuisse Faculty, University of Bern, Bern, Switzerland*

[5] *COMPATH, Vetsuisse Faculty & Faculty of Medicine, University of Bern, Bern, Switzerland*

[*] **Contact:**

marco.alves@vetsuisse.unibe.ch

Phone: +41 31 631 2483

Authors contribution

All authors contributed to important elements to the work presented in this paper and reviewed and approved the final version of this manuscript. T.D. designed the various antibody combination staining, validated them *in vitro*, designed and performed the

animal trials, performed the RSV quantifications in animal tissues and serum micro-neutralization assays, acquired, assembled, analyzed and interpreted the data, prepared the figures and wrote the manuscript. M.B. and B.Z established the RSV quantification and serum micro-neutralization assay protocols and designed and performed the animal trial. B.I.O.E. participated in the execution of the animal trial. K.M. and H.P. participated in the execution of the animal trial and evaluated the lung pathology. A.F. assisted in the animal trial and performed part of the immunohistochemistry. L.B. computed the data from WBC and PMN counts in the circulation with the R software and generated the related figures. C.B. helped with clinical observations, interpretation of the data, and reviewed the manuscript. N.R. participated in the design and execution of the animal trial, organized the partitioning of animals in stables, and monitored the clinical scores. M.P.A. conceived the idea, overviewed, designed, led and performed the animal trial, and edited the manuscript.

Sources of support

The RSV isolate RSV-ON1-H1 was kindly provided by Sibylle Haid, Martin Wetzke, Gesine Hansen and Thomas Pietschmann. T.D. was supported in part by the EU FP7 Project UniVax (HEALTH-F3-2013-60173). This project was funded by the Swiss National Science Foundation (grant No. 310030_172895 to M.P.A.).

Running Title: Atypical neonatal immune response to RSV infection

Abstract word count: 249

Total word count: 3863

Abstract

Rationale. Respiratory syncytial virus (RSV) is a major cause of lower respiratory tract infection in infancy, potentially aided by an inappropriate immune response. Sparse information is available for the distal lung, mostly because data arose from non-invasive samplings of peripheral blood and nasal aspirates.

Objectives. To determine the neonatal immune response to RSV in the bronchoalveolar space and better understand why neonates are at greater risk of developing severe disease.

Methods. We used the newborn lamb, a state-of-the-art translational model of human RSV infection, offering ease sampling and full accessibility to lower airways. Using a multiparameter flow cytometry assay, we evaluated the frequency and activation/maturation state of the major subsets of the developing T-cell compartment.

Measurements and Main Results. The T-cell compartment of the healthy developing lung was very distinct to that seen in adults. We observed a high frequency of type 2 $CD4^+$ (Th2) and $CD8^+$ (Tc2) T-cells, both being a large source of IL-4, which declined progressively over time. Remarkably, RSV infection exacerbated this pro-type 2 environment, rather than inducing a type 2 response *per se*. Neonatal regulatory T-cell (Treg) suppressive functions occurred very early to dampen those Th2 and Tc2 responses, while $\gamma\delta$ T-cells dropped and failed to produce IL-17. The disease severity was related to the magnitude of these T-cell responses.

Conclusion. The atypical neonatal immune response to RSV consists of distinct T-cell subsets that tightly cooperate, namely a combined bronchoalveolar influx of Treg, Th2 and Tc2 cells, associated with a depletion of γδ T-cells.

Keywords: Respiratory syncytial virus; neonatal immunity; bronchiolitis; immunopathogenesis; T cells immunity

Introduction

The human respiratory syncytial virus (RSV) is a seasonal virus, known as the major cause of lower respiratory tract infection during early childhood (1, 2). Worldwide, RSV leads to around 160'000 deaths each year (3). Although there are risk factors for RSV severity such as prematurity and congenital heart disease, the majority of hospitalized infants are previously healthy (4-7), suggesting that the disease is partially linked to inherent properties of early life immunity. The precise understanding of the immune-driven susceptibility of neonates is essential, considering there is no licensed vaccine and available prophylactic treatments are mostly based on palivizumab, a neutralizing antibody used in high-risk group infants (8).

The first exposure to pathogens occurs during the early postnatal period and is critical for lung colonization by immune cells. There is increasing evidence that the overall neonatal T-cell compartment is distinctive during this temporal window (9). Upon stimulation neonatal T-cells tend to differentiate into regulatory T-cells (Tregs), to facilitate self-tolerance to developing organs (10). Also, the developing lung is characterized by a type 2 immune phenotype, and the pulmonary T-cell responses present a T helper type 2 (Th2) bias (11, 12). Remarkably, neonatal $\gamma\delta$ T-cells, a T-cell subset enriched at mucosal barrier sites, have an impaired capacity to respond to stimulation (13-16).

Due to the aforementioned reasons, young infants do not mount a classical pulmonary immune response to pathogens such as RSV, which may contribute to high morbidity and mortality (17, 18). A likely explanation could be a combined contribution of viral load (19) and an inappropriate and/or dysfunctional immune response, through an over-exuberant inflammatory response or a biased T-cell response (9, 20, 21). Neonatal T-cells may have both protective and harmful effects in responses to RSV

infection. While children with T-cell deficiencies cannot efficiently clear the virus (22, 23), it remains controversial whether the severity of RSV disease is associated with a bias towards type 2 cytokines such as IL-4 (24-26).

Knowledge of the course of RSV disease is still limited due to ethical and technical difficulties associated with the investigation of the immune response in human neonates. The neonatal lamb model of RSV infection recapitulates most of the features of paediatric disease. Indeed, RSV is a natural pathogen of ruminants. Experimentally-infected animals clinically present rhinitis, coughing and respiratory distress. Typical pulmonary lesions are bronchiolitis and interstitial pneumonia associated with inflammatory infiltrates (27-29). This model, immunologically related to human, was exploited to have full access to the small airways and follow the pulmonary immune cell features over the course of RSV disease.

Materials and methods

Virus

RSV-A2 strain was obtained from the American Type Culture Collection (ATCC® VR-1540™). RSV-ON1-H1 strain was isolated from nasopharyngeal aspirates of a child below the age of five years with confirmed RSV infection, hospitalized at Hannover Medical School, Germany. The caregivers gave informed consent for sampling and all steps were conducted in compliance with good clinical and ethical practice and approved by the local ethical committee (permission number 63090/2012) (30). Virus propagation and titre determination used standard methods, described in the online supplement.

82 ***Animals***

83 The experiments were approved by the cantonal veterinary authority, and performed
84 in compliance with the Swiss animal protection law under the authorization BE125/17.
85 Animals were housed in the high containment animal facility. *Postpartum*, the
86 acclimatization lasted 3-6 days before infection. In accordance with the principles of
87 the 3Rs, suckling lambs were held together with their mothers and fed *ad libitum*. More
88 details about the housing are given in the online supplement.

89 The transtracheal RSV inoculation was performed under sedation and analgesia by
90 intramuscular injection of a mixture of midazolam (Dormicum®, Roche) 0.2 mg/kg and
91 butorphanol (Morphasol®, Dr. E. Graeub AG) 0.2 mg/kg. The trachea was punctured
92 between the proximal tracheal rings with a 20G needle and a volume of 2 ml of virus
93 (10^8 PFU for RSV-A2; 10^7 PFU for RSV-ON1-H1) or PBS (mock-treated controls) were
94 injected slowly.

95

96 **Histopathology and Immunohistochemistry**

97 The methods used in the present work were described elsewhere (31).

98

99 ***Cell suspension preparation***

100 Cell isolation used standardized methods, described in the online supplement.

101

102 ***Human RSV neutralization assay***

103 Serum neutralization assay used standardized methods, described in the online
104 supplement.

105

106 ***RNA isolation and quantitative PCR***

107 The primer and probe sequences used to detect RSV have been previously described
108 (32).
109
110 ***Flow cytometry***
111 The different ovine immune cell subtypes were identified by flow cytometry (FCM)
112 using an eight-step, seven-color staining protocols. All antibodies used for the
113 procedure, as well as their clones, host, working dilution, and references, are listed in
114 Table E1. Combination stainings analyzed plasmacytoid dendritic cell (pDC), $\gamma\delta$ T-
115 cells, Tregs, CD4 and CD8 T-cell subsets. For the acquisitions, 10^6 events were
116 accumulated for each sample. The experimental schedule is summarized in Table E2.
117 For the counts of cell subtypes, we calculated the ratio (number of events in the gated
118 cell subtype) to (number of all events, excepting cell aggregates and debris). FCM
119 acquisitions were performed on a FACS Canto II (BD Bioscience) using the DIVA
120 software and further analyzed with FlowJo (TreeStar).
121
122 ***Statistical Analysis***
123 Statistical analysis was done using GraphPad Prism 8 software. To determine
124 differences between two groups, non-parametric paired Wilcoxon tests or Mann–
125 Whitney U-tests were used as appropriate. Associations were tested using the
126 Spearman rank correlation test. A $p<0.05$ was considered significant.
127
128
129
130
131

132 ## Results

133 **Respiratory disease following neonatal RSV infection**

134 Selected time-points were as follow: 3 and 6 days post-infection (p.i.), to evaluate the
135 innate and early adaptive responses; 14 days p.i. to assess the adaptive mechanisms
136 and virus clearance; 42 days p.i. to investigate the impact of RSV infection on the
137 immune cell colonization of the developing lung. As controls, non-infected newborns
138 and adults were used (Figure 1A).

139 We quantified RSV in BALs (cellular and fluid fractions) and in the lung tissue.
140 Although RSV clearance was slower in the cellular fraction of BALs, it became
141 undetectable in any sample at day 42 p.i., demonstrating an efficient clearance (Figure
142 1B). Immunohistochemistry of lung tissue sections revealed the presence of RSV-
143 antigens in type I pneumocytes and macrophages (Figure 1C).

144 Clinically, RSV infected neonates showed signs of rhinitis with clear nasal discharge,
145 occasional coughing and wheezing. Macroscopical lesions were visible at days 3-6
146 p.i, including failure of pulmonary collapse and focal, dark-red areas of subpleural
147 pulmonary consolidation and atelectasis. Histological lesions, present at days 3-6 p.i
148 consisted of multifocal-coalescing areas of lymphocytic and histiocytic infiltrates within
149 interalveolar septae (interstitial pneumonia) and accumulation of inflammatory cells
150 within alveolar spaces and bronchioles (bronchiolitis) (Figure 1D). Longitudinal
151 measurements of white blood counts and neutrophil counts in the circulation showed
152 no difference between mock and infected neonates (Figure E1).

153

154 **Neonatal RSV infection activates the initiators of the adaptive immune response**

155 When quantified in the BALs, pDC numbers of mock neonates were similar to those
156 of healthy adults. Upon RSV infection, we observed a trend to pDC recruitment as

157 early as 3 days p.i., and this was enhanced at day 6 p.i. ($p<0.05$). However, this pDC
158 recruitment was transitional and tightly regulated, since day 14 p.i corresponded to a
159 return to steady-state levels (Figure 2A,B). One out of six infected neonates failed to
160 display any pDC recruitment; this animal was the only one for which RSV was
161 undetectable in the fluid fraction of BAL (Figure 1B). To verify whether the extent of
162 pDC recruitment was linked to the magnitude of RSV shedding, pDC counts were
163 plotted as a function of RSV copies in the fluid fraction of BALs. A significant
164 association was found (Figure 2C). We next evaluated if the recruited pDCs displayed
165 a mature and activated phenotype. A significant CD86 upregulation was found at days
166 3-6 p.i. (Figure 2D,E). This upregulation was transitional and back to steady-state
167 levels at day 14 p.i.
168
169 **Neonatal RSV infection leads to a transient depletion of γδ T-cells**
170 γδ T-cell potential impairment in the bronchoalveolar space could contribute to RSV
171 immunopathogenesis (13-15). Their numbers in the BALs of mock neonates were
172 comparable to those of healthy adults. However, RSV infection led to a significant
173 decrease in γδ T-cell frequency at day 14 p.i.. Nevertheless, this γδ T-cell depletion
174 was entirely reversed at day 42 p.i. (Figure 2F,G). To exclude the possibility that the
175 γδ T-cell reduction could be due to migration or relocation, we calculated their counts
176 as a function of the percentage of Live/Dead-positive cells. A negative association was
177 found, suggesting that neonatal γδ T-cells death is linked to the presence of RSV in
178 the bronchoalveolar space (Figure 2H). Finally, BAL γδ T-cells collected from infected
179 neonates failed to produce detectable levels of IL-17.
180 We next ascertained whether neonatal γδ T-cells are characterized by an immature
181 phenotype. Remarkably, in BALs of healthy adults, half of the γδ T-cell pool was

182 composed of mature CD25$^+$ cells, whereas the latter were absent in mock neonates
183 at day 3. The proportion of mature γδ T-cells progressively strengthened over time,
184 without reaching the level detected in healthy adults. RSV infection exerts an effect on
185 this maturation of neonatal γδ T-cells. Not only the observed depletion was rapidly
186 followed by a complete replenishment at day 42 p.i., but also the restoration was
187 accompanied by a marked increase in the percentage of CD25-positive cells,
188 compared to mock neonates (Figure 2I,J).
189
190 **Neonatal RSV infection exacerbates the type 2 cytokine environment**
191 Assessment moved on to adaptive immune response, and more particularly to IL-4
192 *versus* IFN-γ production by T-cells (Figure 3A). In BALs, mock neonates had a very
193 low number of CD4$^+$ and CD8$^+$ T-cells compared to healthy adults. RSV infection led
194 to their strong recruitment, albeit with distinct kinetics. An unexpected reduction of
195 CD4$^+$ T-cell recruitment was seen as soon as 14 days p.i. This contradicted the values
196 obtained for CD8$^+$ T-cells, where the significant enhancement following RSV infection
197 was maintained. When we considered both CD4$^+$ and CD8$^+$ fractions at a later time-
198 point, the numbers were comparable to those of mock neonates (Figure 3B).
199 Surprisingly, mock neonates had high frequencies of Th2 cells, which declined
200 progressively over time. Elevated amounts of spontaneous produced IL-4 were a
201 signature of the developing CD4$^+$ fraction, since it was no longer detectable at day 42,
202 or in healthy adults. Upon infection, this analysis revealed a trend towards an increase
203 in the frequency of those Th2 cells, whereas there was no consistent influence on IFN-
204 γ induction (Figures 3C,D). Consequently, RSV infection in early life exacerbates the
205 overall lung pro-Th2 cytokine environment, rather than inducing a Th2 immune
206 response *per se*.

207 High frequencies of IL-4-expressing $CD8^+$ T-cells (Tc2) were also found in mock
208 neonates. Again, a progressive decline of Tc2 cells occurred up to day 42 p.i.,
209 comparable to negligible levels measured in healthy adults. RSV disease induced a
210 greater overall Tc2-derived cytokine environment in BALs. This exacerbation was
211 tightly regulated, reduced to a level similar to healthy adults at day 14 p.i. Again, no
212 consistent influence of RSV infection was seen on IFN-γ induction (Figure 3E,F).
213 Altogether, these results highlight the role of Tc2 cells as an important source of IL-4
214 production during neonatal RSV infection.
215 We then tested the activation and differentiation of naïve T lymphocytes into memory
216 subsets. The most striking observation was achieved at day 42 p.i.; the percent
217 contributions of different subsets seen in RSV-infected neonates was highly
218 superimposable to that found in healthy adults. This was not the case for mock
219 neonates who had lower frequencies of activated memory T-cells, particularly for the
220 $CD8^+$ fraction (Figure 3G). Consequently, RSV infection in early life modulates the
221 activation and the maturation of the T-cell pool.
222 Next, we monitored the presence of RSV neutralizing antibodies (NAb) (Figures 3H,
223 E2). In the serum of healthy adults and mock neonates, no RSV neutralizing antibodies
224 were detected. In contrast, RSV-infected neonates have naturally acquired NAb at day
225 13-14 p.i., except one animal. Notably, two siblings had RSV NAb preceding infection;
226 this was passively transmitted by their mother whose serum also had a strong RSV-
227 neutralization (Figure E3). We extended the assay to later time points to test the
228 persistence of RSV neutralization. No loss of humoral memory was measured up to
229 42 days p.i (Figure 3I). Altogether, these results indicate that despite an inappropriate
230 cell-mediated immune response, neonates can clear RSV by mounting an efficient
231 humoral response.

232

233 **Neonatal RSV infection rapidly induces Treg suppressive functions to dampen**
234 **the Th2 and Tc2 responses**

235 The shortened kinetics observed for $CD4^+$ T-cells was elaborated by determining
236 whether this was due to an early Treg rather than a classical $CD4^+$ T-cell response
237 (Figure 4A). RSV infection elicited a rapid Treg recruitment in BALs that mirrored the
238 one previously observed for $CD4^+$ T-cells. This Treg dynamic is specific for the airway
239 mucosa, since Treg frequencies remained unchanged in the lung tissue (Figure 4B).
240 We then noticed a trend for Treg subset overrepresentation following RSV infection
241 (Figure 4C). The proportion of Tregs declined progressively over time, tending towards
242 similar levels to those detected in healthy adults. RSV infection promoted
243 enhancement of TGF-β production by Tregs, however not significant (Figure 4D).
244 When Treg counts were calculated as a function of non-Treg $CD4^+$ counts, an
245 association was found, suggesting that $CD4^+$ T-cell pool tends to differentiate into
246 Tregs. When Treg counts were calculated as a function of $CD8^+$ counts, an association
247 was still found, confirming that $CD8^+$ T-cells and Tregs colonized the alveolar space
248 in a coordinated manner. By plotting $CD8^+$ count as a function of non-Tregs $CD4^+$
249 counts, it appeared that T-cell response was mainly driven by the $CD8^+$ fraction (high
250 numbers at days 6 and 14 p.i.) (Figure 4E). In peribronchial LNs following RSV
251 infection, $CD8^+$ counts remained stable over the course of the disease, showing that
252 their accumulation is airway mucosa-specific (Figure 4F). Moreover, unlike the
253 situation described for the BAL compartment, RSV infection did not promote a further
254 increase of Tc2 cells (Figure 4G).

255

256 **Distinct cellular immune response in neonates compare to adults following RSV**
257 **infection**

258 We followed the same approach to dissect the cellular immune response in RSV-
259 infected adults. While the virus clearance was comparable between adults and
260 neonates (Figure 5A), respiratory lesions were absent in adults (Figure 5B).

261 The rapid and robust pDC recruitment observed in infected neonates did not occur in
262 infected adults. However, lung-resident pDCs of the latter were prompt to react,
263 displaying an even more mature and activated phenotype Importantly, this mature
264 pDC response was also tightly regulated (Figure 5C,D).

265 The strong decrease in γδ T-cell counts observed in infected neonates was absent in
266 adults. Moreover, adult γδ T-cells produced high amounts of IL-17, suggesting that IL-
267 17-mediated immunity is deficient in early life (Figure 5E,F) (15). This IL-17 response
268 was accompanied by an activated phenotype, as indicated by the enhanced proportion
269 of $CD25^+$ cells (Figure 5G). From these results, we could ascertain that neonates lack
270 a mature and functional γδ T-cell pool in the lower airways.

271 For the $CD4^+$ compartment, no significant recruitment was found (Figure 5H). The
272 percentage of IL-4-producing cells was very low, and RSV infection had no consistent
273 influence on IFN-γ induction (Figure 5I). Another clear difference was the contraction
274 of effector memory pool ($CD25^+CD45RO^+$) at day 14 p.i., indicative of a specific
275 immune response (Figure 5J).

276 The recruitment of $CD8^+$ T-cells was delayed compared to neonates, only detectable
277 at day 14 p.i. (Figure 5K). Again, the percentage of IL-4-producing cells was low
278 (Figure 5L), whereas the precipitous contraction of effector memory pool at day 14 p.i.
279 suggested a RSV-specific $CD8^+$ T-cell response (Figure 5M). From these results, it

280 became clear that the inaptitude of neonates to mount an effector T-cell response is
281 tentatively substituted by a fast and massive Th2/Tc2 cell recruitment.
282 Finally, we failed to detect any Treg recruitment. However, the rare tissue-resident
283 Tregs were able to produce TGF-β, suggesting that an immune regulation happened
284 (Figure 5N,O).
285
286 **The severity of disease relates to the magnitude of bronchoalveolar T-cell**
287 **responses**
288 The pulmonary T-cell response was evaluated in neonates infected with RSV-ON1-
289 H1 strain, which induced a milder disease (Figure 6A). We did not observe a γδ T-cell
290 depletion, and the $CD8^+$ T-cell recruitment was delayed. Furthermore, the Treg
291 recruitment was lower compared to RSV A2 infection (Figure 6B). By combining
292 results obtained with both strains, we found a significant association between Treg
293 and pDC counts in BALs (Figure 6C). This indicates that, despite their skew, all distinct
294 subsets of neonatal T-cells cooperate tightly with the magnitude of the cellular immune
295 response against RSV infection.
296
297
298 ## Discussion
299 To properly assess the immunopathogenesis of RSV, it is essential to select a model
300 that recapitulates the features of human disease. We selected the neonatal lamb, as
301 RSV is a natural pathogen for this species, lung development is similar, and the key
302 features mimic human RSV infection in infants (27, 28). One strength of our
303 experimental approach was the ease sampling and the full accessibility to the lower
304 airways throughout the disease when sampling in infants is mainly restricted to the

305 upper airways, the latter representing only an approximate surrogate of the distal lung
306 where RSV disease occurs. Moreover, we offer an unprecedented view of the
307 development of pulmonary neonatal immunity in healthy conditions. This process is
308 highly dynamic and tightly regulated, with a short and early stage where colonizing T-
309 cell subsets synergize towards a narrow pro-tolerogenic window, namely a
310 "Treg/Th2/Tc2" environment. This certainly contributes to the maturation of the
311 immune system and may constitute an unsuitable state to resolve RSV infection.
312 The mechanisms underlying the severity of disease are still unclear. Herein, we
313 observed a comparable virus clearance between adults and neonates, reinforcing the
314 assumption of an inappropriate immune response. We observed a rapid and robust
315 recruitment of neonatal pDCs, whose extent correlated with the viral loads of infected
316 neonates. Infected adults did not require this recruitment, since their lung-resident
317 pDCs reacted promptly by maturing to a higher level than that measured in neonates.
318 This partially corroborates recent studies reporting low counts and maturation levels
319 of pDCs in mice and infants (33, 34). This reduced capacity to respond against RSV
320 might be due to a direct disturbance of signaling by RSV itself (35), or an intrinsic
321 deficiency of neonatal pDCs to produce elevated amounts of cytokines (36-38). This
322 neonatal defect would prevent conventional DCs from adequate presentation of viral
323 antigens, contributing to poor specific T-cell responses (39).
324 Controversial is whether γδ T-cells participate in viral clearance or immunopathology.
325 Herein, the γδ T-cell depletion conflicted with a previous report. Indeed, children with
326 severe RSV bronchiolitis had reduced frequencies of γδ T-cells in peripheral blood,
327 which was explained by the authors as a likely redistribution towards the lungs;
328 unfortunately, they could not evaluate their hypothesis (40). In line with our findings,
329 mice depleted of γδ T-cells before RSV infection display increased viral titers (13). An

330 alternative hypothesis that would reconcile our study with others, is that γδ T-cell tissue
331 redistribution plays less of a role than its immature state in early life. Peripheral blood
332 γδ T-cells of infants with severe disease failed to produce IFN-γ when restimulated
333 (14), whereas γδ T-cells from neonatal mice had an impaired ability to produce IL-17
334 (15). Finally, Tc17 and Th17 cells were recently associated with shorter hospital stays
335 and proposed to play a protective role (26). Altogether, our data demonstrate that the
336 protective role of γδ T-cells in RSV infection is largely inefficient in early life.
337 The BALs of neonates displayed a high proportion of Tregs that declined rapidly to
338 levels comparable to healthy adults. As fetal $CD4^+$ T-cells tend to differentiate
339 preferentially into Tregs after stimulation (10), this tolerogenic mechanism is likely to
340 promote self-tolerance to the developing lung. We found that Treg response to RSV
341 infection happened very early in neonates, accompanying $CD4^+$ and $CD8^+$ T-cell
342 expansion rather than shutting them down afterwards. This strong Treg recruitment
343 was absent in adults. We speculate that the neonate immune system faces a dilemma
344 between avoiding potential autoimmune disorders and failing to mount a specific T-
345 cell response to harmful pathogens. Studies conducted in young infants with RSV
346 disease support this statement. A selective depletion of peripheral Tregs was shown,
347 probably due to massive recruitment to the lungs (41). A higher level of TGF-β
348 transcript was measured in neonatal DCs compared to adults (42). In contrast, some
349 reports emphasized the protective role of Tregs, since Treg-depleted young mice had
350 an enhanced RSV disease, with abundant T-cells exhibiting an activated phenotype
351 (43). Another remarkable observation was the strong correlation between pDC and
352 Treg counts. Despite the need for further investigations, it is worth noting that pDC to
353 Treg ratio was linked to the clearance *versus* persistence of human papillomavirus
354 (44).

355 Whether the cellular arm of the adaptive pulmonary response is detrimental or
356 beneficial in RSV disease is still debated. Particularly, the contribution of IL-4 to viral
357 clearance versus immunopathogenesis remains controversial (25, 45-47). Recently, a
358 study performed in hospitalized infants showed a possible involvement of Tc2 cells in
359 disease severity. Although convincing, this study was for obvious ethical reasons
360 restricted to nasal aspirates (26). Interestingly, Tc2 cells are increasingly proposed to
361 play an important role in the etiology of asthma (48). Herein, we provide a significant
362 advancement in understanding this yet unclear IL-4 contribution, by showing that type
363 2 cytokine environment in the lung is a footprint of early life that decreases rapidly with
364 time in healthy conditions. RSV infection circumvents this decline by mediating the
365 massive recruitment of $CD4^+$ and $CD8^+$ T-cells, exacerbating the overall type 2
366 cytokine environment. We think that the link between IL-4 and RSV disease is the
367 direct consequence of a strong trafficking of endogenous Th2 and Tc2 lymphocytes
368 towards infected pulmonary tissues, rather than an RSV-specific type 2 immune
369 response *per se*.
370 The high proportion of pulmonary T-cells producing spontaneously IL-4 was
371 undetectable in the healthy adults. Neither was the RSV-specific immune response of
372 adults oriented towards a Th2 or Tc2 profile. This corroborates a previous report
373 mentioning an endogenously poised cytokine profile toward IL-4 in $CD4^+$ T-cells in
374 cord blood of neonates and infants, establishing a link between IL-4 and development
375 (49). However, we provide new insights by demonstrating that i) $CD8^+$ Tc2 cells are
376 an equal and possibly superior source of IL-4 than $CD4^+$ Th2 cells; ii) this
377 immunological state occurs during a short period *in vivo*, raising the likelihood that
378 numerous animal trials failed to detect it due to the study design. Remarkably, this
379 transient type 2 cytokine environment was exacerbated upon RSV infection. So far,

380 similar observations were only made at the systemic level or in nasal aspirates, and
381 authors could only speculate on the relocation to the lower respiratory tract (26, 50).
382 Herein, not only we show that this happens, but we also unify the link between IL-4
383 and RSV disease and endogenous IL-4 program in neonates. This finding constitutes
384 an important step towards deciphering why neonates and young infants are
385 particularly at risk.
386

387 **Conclusion**

388 Our holistic approach provided novel insights into the identification of the host's
389 contributing factors to RSV immunopathology, strengthening the hypothesis of an
390 inappropriate immune response in the narrow temporal window of early life. This can
391 now be characterized as a combined bronchoalveolar influx of Treg, Th2 and Tc2 cells,
392 associated with a strong depletion of $\gamma\delta$ T-cells. These findings constitute a novel basis
393 for further exploration of RSV immunopathogenesis and should be considered in RSV
394 vaccine design, which remains challenging after five decades of effort.

Acknowledgements

We thank Artur Summerfield, Christoph Aebi and Sean R. R. Hall for helpful discussions; Sylvie Python and Aurélie Godel for technical assistance; Inês Berenguer Veiga for participation in the animal trial; Hans Peter Lüthi, Roman Troxler, Jan Salchli, Daniel Brechbühl and Katarzyna Sliz for animal care.

400 ## References

401

402 1. Shi T, McAllister DA, O'Brien KL, Simoes EAF, Madhi SA, Gessner BD, Polack FP, Balsells
403 E, Acacio S, Aguayo C, Alassani I, Ali A, Antonio M, Awasthi S, Awori JO, Azziz-
404 Baumgartner E, Baggett HC, Baillie VL, Balmaseda A, Barahona A, Basnet S, Bassat
405 Q, Basualdo W, Bigogo G, Bont L, Breiman RF, Brooks WA, Broor S, Bruce N, Bruden
406 D, Buchy P, Campbell S, Carosone-Link P, Chadha M, Chipeta J, Chou M, Clara W,
407 Cohen C, de Cuellar E, Dang DA, Dash-Yandag B, Deloria-Knoll M, Dherani M, Eap
408 T, Ebruke BE, Echavarria M, de Freitas Lazaro Emediato CC, Fasce RA, Feikin DR,
409 Feng L, Gentile A, Gordon A, Goswami D, Goyet S, Groome M, Halasa N, Hirve S,
410 Homaira N, Howie SRC, Jara J, Jroundi I, Kartasasmita CB, Khuri-Bulos N, Kotloff KL,
411 Krishnan A, Libster R, Lopez O, Lucero MG, Lucion F, Lupisan SP, Marcone DN,
412 McCracken JP, Mejia M, Moisi JC, Montgomery JM, Moore DP, Moraleda C, Moyes J,
413 Munywoki P, Mutyara K, Nicol MP, Nokes DJ, Nymadawa P, da Costa Oliveira MT,
414 Oshitani H, Pandey N, Paranhos-Baccala G, Phillips LN, Picot VS, Rahman M, Rakoto-
415 Andrianarivelo M, Rasmussen ZA, Rath BA, Robinson A, Romero C, Russomando G,
416 Salimi V, Sawatwong P, Scheltema N, Schweiger B, Scott JAG, Seidenberg P, Shen
417 K, Singleton R, Sotomayor V, Strand TA, Sutanto A, Sylla M, Tapia MD, Thamthitiwat
418 S, Thomas ED, Tokarz R, Turner C, Venter M, Waicharoen S, Wang J,
419 Watthanaworawit W, Yoshida LM, Yu H, Zar HJ, Campbell H, Nair H, Network RSVGE.
420 Global, regional, and national disease burden estimates of acute lower respiratory
421 infections due to respiratory syncytial virus in young children in 2015: a systematic
422 review and modelling study. *Lancet* 2017; 390: 946-958.

423 2. Pneumonia Etiology Research for Child Health Study G. Causes of severe pneumonia
424 requiring hospital admission in children without HIV infection from Africa and Asia: the
425 PERCH multi-country case-control study. *Lancet* 2019; 394: 757-779.

426 3. Nair H, Nokes DJ, Gessner BD, Dherani M, Madhi SA, Singleton RJ, O'Brien KL, Roca A,
427 Wright PF, Bruce N, Chandran A, Theodoratou E, Sutanto A, Sedyaningsih ER,
428 Ngama M, Munywoki PK, Kartasasmita C, Simoes EA, Rudan I, Weber MW, Campbell
429 H. Global burden of acute lower respiratory infections due to respiratory syncytial virus
430 in young children: a systematic review and meta-analysis. *Lancet* 2010; 375: 1545-
431 1555.
432 4. Hall CB, Weinberg GA, Iwane MK, Blumkin AK, Edwards KM, Staat MA, Auinger P, Griffin
433 MR, Poehling KA, Erdman D, Grijalva CG, Zhu Y, Szilagyi P. The burden of respiratory
434 syncytial virus infection in young children. *N Engl J Med* 2009; 360: 588-598.
435 5. Murray J, Bottle A, Sharland M, Modi N, Aylin P, Majeed A, Saxena S, Medicines for
436 Neonates Investigator G. Risk factors for hospital admission with RSV bronchiolitis in
437 England: a population-based birth cohort study. *PLoS One* 2014; 9: e89186.
438 6. Garcia CG, Bhore R, Soriano-Fallas A, Trost M, Chason R, Ramilo O, Mejias A. Risk factors
439 in children hospitalized with RSV bronchiolitis versus non-RSV bronchiolitis. *Pediatrics*
440 2010; 126: e1453-1460.
441 7. Hall CB, Weinberg GA, Blumkin AK, Edwards KM, Staat MA, Schultz AF, Poehling KA,
442 Szilagyi PG, Griffin MR, Williams JV, Zhu Y, Grijalva CG, Prill MM, Iwane MK.
443 Respiratory syncytial virus-associated hospitalizations among children less than 24
444 months of age. *Pediatrics* 2013; 132: e341-348.
445 8. Palivizumab, a Humanized Respiratory Syncytial Virus Monoclonal Antibody, Reduces
446 Hospitalization From Respiratory Syncytial Virus Infection in High-risk Infants.
447 *Pediatrics* 1998; 102: 531-537.
448 9. Openshaw PJM, Chiu C, Culley FJ, Johansson C. Protective and Harmful Immunity to RSV
449 Infection. *Annu Rev Immunol* 2017; 35: 501-532.
450 10. Mold JE, Venkatasubrahmanyam S, Burt TD, Michaelsson J, Rivera JM, Galkina SA,
451 Weinberg K, Stoddart CA, McCune JM. Fetal and adult hematopoietic stem cells give
452 rise to distinct T cell lineages in humans. *Science* 2010; 330: 1695-1699.

453 11. de Kleer IM, Kool M, de Bruijn MJ, Willart M, van Moorleghem J, Schuijs MJ, Plantinga M,
454 Beyaert R, Hams E, Fallon PG, Hammad H, Hendriks RW, Lambrecht BN. Perinatal
455 Activation of the Interleukin-33 Pathway Promotes Type 2 Immunity in the Developing
456 Lung. *Immunity* 2016; 45: 1285-1298.
457 12. PrabhuDas M, Adkins B, Gans H, King C, Levy O, Ramilo O, Siegrist CA. Challenges in
458 infant immunity: implications for responses to infection and vaccines. *Nat Immunol*
459 2011; 12: 189-194.
460 13. Dodd J, Riffault S, Kodituwakku JS, Hayday AC, Openshaw PJ. Pulmonary V gamma 4+
461 gamma delta T cells have proinflammatory and antiviral effects in viral lung disease. *J*
462 *Immunol* 2009; 182: 1174-1181.
463 14. Aoyagi M, Shimojo N, Sekine K, Nishimuta T, Kohno Y. Respiratory syncytial virus
464 infection suppresses IFN-gamma production of gammadelta T cells. *Clin Exp Immunol*
465 2003; 131: 312-317.
466 15. Huang H, Saravia J, You D, Shaw AJ, Cormier SA. Impaired gamma delta T cell-derived
467 IL-17A and inflammasome activation during early respiratory syncytial virus infection
468 in infants. *Immunol Cell Biol* 2015; 93: 126-135.
469 16. McGill JL, Sacco RE. gammadelta T cells and the immune response to respiratory
470 syncytial virus infection. *Vet Immunol Immunopathol* 2016; 181: 24-29.
471 17. Restori KH, Srinivasa BT, Ward BJ, Fixman ED. Neonatal Immunity, Respiratory Virus
472 Infections, and the Development of Asthma. *Front Immunol* 2018; 9: 1249.
473 18. Levy O. Innate immunity of the newborn: basic mechanisms and clinical correlates. *Nat*
474 *Rev Immunol* 2007; 7: 379-390.
475 19. DeVincenzo JP, Wilkinson T, Vaishnaw A, Cehelsky J, Meyers R, Nochur S, Harrison L,
476 Meeking P, Mann A, Moane E, Oxford J, Pareek R, Moore R, Walsh E, Studholme R,
477 Dorsett P, Alvarez R, Lambkin-Williams R. Viral load drives disease in humans
478 experimentally infected with respiratory syncytial virus. *Am J Respir Crit Care Med*
479 2010; 182: 1305-1314.

480 20. Pino M, Kelvin DJ, Bermejo-Martin JF, Alonso A, Matias V, Tenorio A, Rico L, Eiros JM,
481 Castrodeza J, Blanco-Quiros A, Ardura J, de Lejarazu RO. Nasopharyngeal aspirate
482 cytokine levels 1 yr after severe respiratory syncytial virus infection. *Pediatr Allergy*
483 *Immunol* 2009; 20: 791-795.
484 21. Johnson JE, Gonzales RA, Olson SJ, Wright PF, Graham BS. The histopathology of fatal
485 untreated human respiratory syncytial virus infection. *Mod Pathol* 2007; 20: 108-119.
486 22. Piedra PA. Clinical experience with respiratory syncytial virus vaccines. *Pediatr Infect Dis*
487 *J* 2003; 22: S94-99.
488 23. Fishaut M, Tubergen D, McIntosh K. Cellular response to respiratory viruses with particular
489 reference to children with disorders of cell-mediated immunity. *J Pediatr* 1980; 96: 179-
490 186.
491 24. Roman M, Calhoun WJ, Hinton KL, Avendano LF, Simon V, Escobar AM, Gaggero A, Diaz
492 PV. Respiratory syncytial virus infection in infants is associated with predominant Th-
493 2-like response. *Am J Respir Crit Care Med* 1997; 156: 190-195.
494 25. Legg JP, Hussain IR, Warner JA, Johnston SL, Warner JO. Type 1 and type 2 cytokine
495 imbalance in acute respiratory syncytial virus bronchiolitis. *Am J Respir Crit Care Med*
496 2003; 168: 633-639.
497 26. Siefker DT, Vu L, You D, McBride A, Taylor R, Jones TL, DeVincenzo J, Cormier SA.
498 Respiratory Syncytial Virus Disease Severity Is Associated with Distinct CD8(+) T-Cell
499 Profiles. *Am J Respir Crit Care Med* 2020; 201: 325-334.
500 27. Olivier A, Gallup J, de Macedo MM, Varga SM, Ackermann M. Human respiratory syncytial
501 virus A2 strain replicates and induces innate immune responses by respiratory
502 epithelia of neonatal lambs. *Int J Exp Pathol* 2009; 90: 431-438.
503 28. Sitthicharoenchai P, Alnajjar S, Ackermann MR. A model of respiratory syncytial virus
504 (RSV) infection of infants in newborn lambs. *Cell Tissue Res* 2020; 380: 313-324.
505 29. Derscheid RJ, Ackermann MR. Perinatal lamb model of respiratory syncytial virus (RSV)
506 infection. *Viruses* 2012; 4: 2359-2378.

507 30. Blockus S, Sake SM, Wetzke M, Grethe C, Graalmann T, Pils M, Le Goffic R, Galloux M,
508 Prochnow H, Rox K, Huttel S, Rupcic Z, Wiegmann B, Dijkman R, Rameix-Welti MA,
509 Eleouet JF, Duprex WP, Thiel V, Hansen G, Bronstrup M, Haid S, Pietschmann T.
510 Labyrinthopeptins as virolytic inhibitors of respiratory syncytial virus cell entry. *Antiviral*
511 *Res* 2020; 177: 104774.
512 31. Mehinagic K, Pilo P, Vidondo B, Stokar-Regenscheit N. Coinfection of Swiss cattle with
513 bovine parainfluenza virus 3 and Mycoplasma bovis at acute and chronic stages of
514 bovine respiratory disease complex. *J Vet Diagn Invest* 2019; 31: 674-680.
515 32. Lee DC, Harker JA, Tregoning JS, Atabani SF, Johansson C, Schwarze J, Openshaw PJ.
516 CD25+ natural regulatory T cells are critical in limiting innate and adaptive immunity
517 and resolving disease following respiratory syncytial virus infection. *J Virol* 2010; 84:
518 8790-8798.
519 33. Kerrin A, Fitch P, Errington C, Kerr D, Waxman L, Riding K, McCormack J, Mehendele F,
520 McSorley H, MacKenzie K, Wronski S, Braun A, Levin R, Theilen U, Schwarze J.
521 Differential lower airway dendritic cell patterns may reveal distinct endotypes of RSV
522 bronchiolitis. *Thorax* 2017; 72: 620-627.
523 34. Ruckwardt TJ, Malloy AM, Morabito KM, Graham BS. Quantitative and qualitative deficits
524 in neonatal lung-migratory dendritic cells impact the generation of the CD8+ T cell
525 response. *PLoS Pathog* 2014; 10: e1003934.
526 35. Johnson TR, Johnson CN, Corbett KS, Edwards GC, Graham BS. Primary human mDC1,
527 mDC2, and pDC dendritic cells are differentially infected and activated by respiratory
528 syncytial virus. *PLoS One* 2011; 6: e16458.
529 36. Kollmann TR, Crabtree J, Rein-Weston A, Blimkie D, Thommai F, Wang XY, Lavoie PM,
530 Furlong J, Fortuno ES, 3rd, Hajjar AM, Hawkins NR, Self SG, Wilson CB. Neonatal
531 innate TLR-mediated responses are distinct from those of adults. *J Immunol* 2009;
532 183: 7150-7160.
533 37. Marr N, Wang TI, Kam SH, Hu YS, Sharma AA, Lam A, Markowski J, Solimano A, Lavoie
534 PM, Turvey SE. Attenuation of respiratory syncytial virus-induced and RIG-I-

535 dependent type I IFN responses in human neonates and very young children. *J*
536 *Immunol* 2014; 192: 948-957.
537 38. Danis B, George TC, Goriely S, Dutta B, Renneson J, Gatto L, Fitzgerald-Bocarsly P,
538 Marchant A, Goldman M, Willems F, De Wit D. Interferon regulatory factor 7-mediated
539 responses are defective in cord blood plasmacytoid dendritic cells. *Eur J Immunol*
540 2008; 38: 507-517.
541 39. Lau-Kilby AW, Turfkruyer M, Kehl M, Yang L, Buchholz UJ, Hickey K, Malloy AMW. Type
542 I IFN ineffectively activates neonatal dendritic cells limiting respiratory antiviral T-cell
543 responses. *Mucosal Immunol* 2020; 13: 371-380.
544 40. De Weerd W, Twilhaar WN, Kimpen JL. T cell subset analysis in peripheral blood of
545 children with RSV bronchiolitis. *Scand J Infect Dis* 1998; 30: 77-80.
546 41. Raiden S, Pandolfi J, Payaslian F, Anderson M, Rivarola N, Ferrero F, Urtasun M,
547 Fainboim L, Geffner J, Arruvito L. Depletion of circulating regulatory T cells during
548 severe respiratory syncytial virus infection in young children. *Am J Respir Crit Care*
549 *Med* 2014; 189: 865-868.
550 42. Thornburg NJ, Shepherd B, Crowe JE, Jr. Transforming growth factor beta is a major
551 regulator of human neonatal immune responses following respiratory syncytial virus
552 infection. *J Virol* 2010; 84: 12895-12902.
553 43. Durant LR, Makris S, Voorburg CM, Loebbermann J, Johansson C, Openshaw PJ.
554 Regulatory T cells prevent Th2 immune responses and pulmonary eosinophilia during
555 respiratory syncytial virus infection in mice. *J Virol* 2013; 87: 10946-10954.
556 44. Strickler HD, Martinson J, Desai S, Xie X, Burk RD, Anastos K, Massad LS, Minkoff H,
557 Xue X, D'Souza G, Levine AM, Colie C, Watts DH, Palefsky JM, Landay A. The relation
558 of plasmacytoid dendritic cells (pDCs) and regulatory T-cells (Tregs) with HPV
559 persistence in HIV-infected and HIV-uninfected women. *Viral Immunol* 2014; 27: 20-
560 25.
561 45. Caballero MT, Serra ME, Acosta PL, Marzec J, Gibbons L, Salim M, Rodriguez A, Reynaldi
562 A, Garcia A, Bado D, Buchholz UJ, Hijano DR, Coviello S, Newcomb D, Bellabarba M,

563 Ferolla FM, Libster R, Berenstein A, Siniawaski S, Blumetti V, Echavarria M, Pinto L,
564 Lawrence A, Ossorio MF, Grosman A, Mateu CG, Bayle C, Dericco A, Pellegrini M,
565 Igarza I, Repetto HA, Grimaldi LA, Gudapati P, Polack NR, Althabe F, Shi M, Ferrero
566 F, Bergel E, Stein RT, Peebles RS, Boothby M, Kleeberger SR, Polack FP. TLR4
567 genotype and environmental LPS mediate RSV bronchiolitis through Th2 polarization.
568 *J Clin Invest* 2015; 125: 571-582.
569 46. Bermejo-Martin JF, Garcia-Arevalo MC, De Lejarazu RO, Ardura J, Eiros JM, Alonso A,
570 Matias V, Pino M, Bernardo D, Arranz E, Blanco-Quiros A. Predominance of Th2
571 cytokines, CXC chemokines and innate immunity mediators at the mucosal level during
572 severe respiratory syncytial virus infection in children. *Eur Cytokine Netw* 2007; 18:
573 162-167.
574 47. Vu LD, Siefker D, Jones TL, You D, Taylor R, DeVincenzo J, Cormier SA. Elevated Levels
575 of Type 2 Respiratory Innate Lymphoid Cells in Human Infants with Severe Respiratory
576 Syncytial Virus Bronchiolitis. *Am J Respir Crit Care Med* 2019; 200: 1414-1423.
577 48. Hinks TSC, Hoyle RD, Gelfand EW. CD8(+) Tc2 cells: underappreciated contributors to
578 severe asthma. *Eur Respir Rev* 2019; 28.
579 49. Hebel K, Weinert S, Kuropka B, Knolle J, Kosak B, Jorch G, Arens C, Krause E, Braun-
580 Dullaeus RC, Brunner-Weinzierl MC. CD4+ T cells from human neonates and infants
581 are poised spontaneously to run a nonclassical IL-4 program. *J Immunol* 2014; 192:
582 5160-5170.
583 50. Bendelja K, Gagro A, Bace A, Lokar-Kolbas R, Krsulovic-Hresic V, Drazenovic V, Mlinaric-
584 Galinovic G, Rabatic S. Predominant type-2 response in infants with respiratory
585 syncytial virus (RSV) infection demonstrated by cytokine flow cytometry. *Clin Exp*
586 *Immunol* 2000; 121: 332-338.
587

588 ## Figure legends

589

590 **Figure 1. Neonatal RSV infection causes bronchiolitis and interstitial**
591 **pneumonia.** (A) Illustration of the transtracheal RSV infection experimental design.
592 (B) RSV was quantified in the respiratory tract (BAL, cell fraction; Lung; BAL, fluid) by
593 qPCR. (C) RSV detection by immunohistochemistry in macrophages, and type I
594 pneumocytes. (D) Representative histological lung tissue sections from neonates over
595 the course of RSV infection (40X, HE). Lungs of RSV-infected animals (strain A2)
596 show interstitial septae expanded by inflammatory cells (interstitial pneumonia) and
597 accumulation of inflammatory cells within alveoli at days 3 and 6 p.i. No lesions at days
598 14 and 42 p.i. The lungs of mock neonates allow comparison with normal lung
599 architecture within the first weeks of life. Each symbol represents an individual animal
600 (healthy adults, n=3; mock neonates, n=3; neonates infected with RSV, n=6). Boxplots
601 indicate median value (center line) and interquartile ranges (box edges), with whiskers
602 extending to the lowest and the highest values. Stars indicate significance levels. *, p
603 < 0.05.

604

605 **Figure 2. Neonatal RSV infection activates the initiators of the adaptive immune**
606 **response and induces a transient depletion of γδ T-cells.** (A-E) Neonatal RSV
607 infection induces bronchoalveolar space recruitment of activated pDCs. (A) FCM
608 gating strategy for ovine pDCs. (B) Neonatal RSV infection induces an early and
609 transient bronchoalveolar space colonization by pDCs. (C) Correlation coefficient (r)
610 obtained with pDC counts calculated as a function of RSV copies/10^{12} 18S copies.
611 Significance was reached for BAL fluid but not for BAL, cell fraction. (D-E) A high
612 frequency of recruited pDCs in bronchoalveolar space upregulate CD86 (D,

613 representative FCM contour plots; E, plot displaying all individuals). (F-J) Neonatal
614 RSV infection leads to the transient depletion of γδ T-cell subset in the bronchoalveolar
615 space, followed by a full replenishment and an accelerated maturation. (F) FACS
616 gating strategy for ovine γδ T-cells. (G) Neonatal RSV infection induces a decrease in
617 γδ T-cells number in the bronchoalveolar space. (H) Correlation coefficient (r) obtained
618 with in γδ T-cell counts calculated as a function of % Live/Dead$^+$. (I-J) Replenishment
619 and maturation (CD25 up-regulation) of γδ T-cell subset following the depletion after
620 RSV infection (I, representative FACS contour plots; J, Pie charts displaying all
621 individuals). Each symbol represents an individual animal (healthy adults, n=3; mock
622 neonates, n=3; neonates infected with RSV, n=6). Boxplots indicate median value
623 (center line) and interquartile ranges (box edges), with whiskers extending to the
624 lowest and the highest values. Stars indicate significance levels. *, $p < 0.05$.
625
626 **Figure 3. Neonatal RSV infection exacerbates the type 2 cytokine environment**
627 **in lung.** (A) FCM gating strategy for ovine CD4$^+$ and CD8$^+$ T-cells. (B) RSV infection
628 in neonate accelerates the recruitment of CD4$^+$ and CD8$^+$ T-cells in the
629 bronchoalveolar space. (C-D) A high frequency of recruited CD4$^+$ T-cells in
630 bronchoalveolar space differentiate towards a Th2 cytokine profile (IL-4 production)
631 (C, representative FACS contour plots; D, plot displaying all individuals). (E-F) A high
632 frequency of recruited CD8$^+$ T-cells in bronchoalveolar space differentiate towards a
633 Tc2 cytokine profile (IL-4 production) (E, representative FCM contour plots; F, plot
634 displaying all individuals). (G) RSV infection in neonates modulates the activation (cell
635 surface expression of CD25) and the maturation (cell surface expression of T-cell
636 memory marker CD45RO) of CD4$^+$ and CD8$^+$ T-cell pools in the lung. (H) Neonates
637 infected with RSV can mount an antiviral neutralizing-antibody response. (I) Anti-RSV

638 Nabs persist over a 42-day long period. Each symbol represents an individual animal
639 (healthy adults, n=3; mock neonates, n=3; neonates infected with RSV, n=6). Boxplots
640 indicate median value (center line) and interquartile ranges (box edges), with whiskers
641 extending to the lowest and the highest values. Stars indicate significance levels. *, p
642 < 0.05; **, $p < 0.01$).
643
644 **Figure 4. Neonatal RSV infection rapidly induces Treg suppressive functions to**
645 **dampen the Th2 and Tc2 responses.** (A) FCM gating strategy for ovine $CD4^+$ and
646 $CD8^+$ T-cells. (B) RSV infection in neonates led to the recruitment of Tregs in the
647 bronchoalveolar space (left panel), but not in the lung (right panel). (C) Progressive
648 decrease with age of Treg subset among the $CD4^+$ T-cell fraction (representative FCM
649 contour plots). (D) Frequency of TGF-β-producing Tregs. (E) Correlation coefficient (r)
650 obtained in BALs with Treg counts calculated as a function of non-Treg $CD4^+$ counts
651 (left), Treg counts calculated as a function of $CD8^+$ counts (middle) and $CD8^+$ counts
652 calculated as a function of non-Treg $CD4^+$ counts (right). Significance was reached for
653 the three correlations. (F) $CD8^+$ T-cell counts remained stable in the peribronchial LNs
654 over the course of neonatal RSV infection. (G) Role of neonatal RSV infection on
655 cytokine production by $CD8^+$ T-cells in draining LNs. Upper panel: poor influence on
656 the frequency of IL-4^+ $CD8^+$ T-cells (representative FCM contour plots). Lower panel:
657 slight, but significant enhancement of IL-17^+ $CD8^+$ T-cells (representative FCM contour
658 plots). Each symbol represents an individual animal (healthy adults, n=3; mock
659 neonates, n=3; neonates infected with RSV, n=6). Boxplots indicate median value
660 (center line) and interquartile ranges (box edges), with whiskers extending to the
661 lowest and the highest values. Stars indicate significance levels. *, $p < 0.05$; **, $p <$
662 0.01.

663

664 **Figure 5. Distinct cellular immune response in neonates compare to adults**
665 **following RSV infection.** (A) RSV was quantified in the respiratory tract (BAL, cell
666 fraction; lung; BAL, fluid) of adults and neonates by qPCR. (B) Representative
667 histological lung tissue sections from RSV-infected neonates and adults at day 6 and
668 14 p.i. (40X, HE). Adults show no histological lesions, whereas neonates show
669 interstitial pneumonia at day 6.p.i. (C-D) Counts of recruited pDCs and CD86
670 upregulation in bronchoalveolar space (C, plot displaying all individuals; D,
671 representative FCM contour plots). (E-G) $\gamma\delta$ T-cell counts, cytokine production, and
672 maturation in the bronchoalveolar space (E, plot displaying all individuals; F,
673 representative FCM contour plots; G, pie charts integrating all animals). (H-J)
674 Recruitment, activation, and maturation of the $CD4^+$ T-cell pool in the bronchoalveolar
675 space (H, plot displaying all individuals; I, representative FACS contour plots; J, pie
676 charts integrating all animals). (K-M) As in (H-J), but showing $CD8^+$ T-cell pool. (N-O)
677 Recruitment of Tregs and TGF-β production in the bronchoalveolar space (N, plot
678 displaying all individuals; O, representative FACS contour plots). Each symbol
679 represents an individual animal (infected adults, n=3; neonates infected with RSV,
680 n=6). The grey zone corresponds to the interval integrating the values of all
681 corresponding mock controls. Boxplots indicate median value (center line) and
682 interquartile ranges (box edges), with whiskers extending to the lowest and the highest
683 values. Stars indicate significance levels. *, $p < 0.05$; **, $p < 0.01$; ***, $p < 0.001$.

684

685 **Figure 6. The severity of disease relates to the magnitude of bronchoalveolar T-**
686 **cell responses.** (A) Representative histological lung tissue sections from mock
687 neonates and neonates infected with RSV-ON1-H1 and RSV A2 strain (40X, HE). At
688 day 6 p.i. the RSV-ON1-H1 infected animals show mild interstitial pneumonia (upper
689 right corner) with accumulation of inflammatory cells within alveoli. No lesions at day
690 14 p.i. or mock-infected animals. (B) Comparison of immune cell subset trafficking into
691 bronchoalveolar space after infection with RSV-ON1-H1 or RSV A2 strains. (C)
692 Correlation coefficient (r) obtained in BALs with Treg counts calculated as a function
693 of pDC counts. Each symbol represents an individual animal (infected adults, n=3;
694 neonates infected with RSV, n=6). The grey zone corresponds to the interval
695 integrating the values of all corresponding mock controls. Boxplots indicate median
696 value (center line) and interquartile ranges (box edges), with whiskers extending to the
697 lowest and the highest values. Stars indicate significance levels. *, $p < 0.05$; **, $p <$
698 0.01; ***, $p < 0.001$.

699

700 **Data availability statement**

701 The data generated and analysed during the current study are available from the
702 corresponding author on reasonable request.

703 **Figure 1**

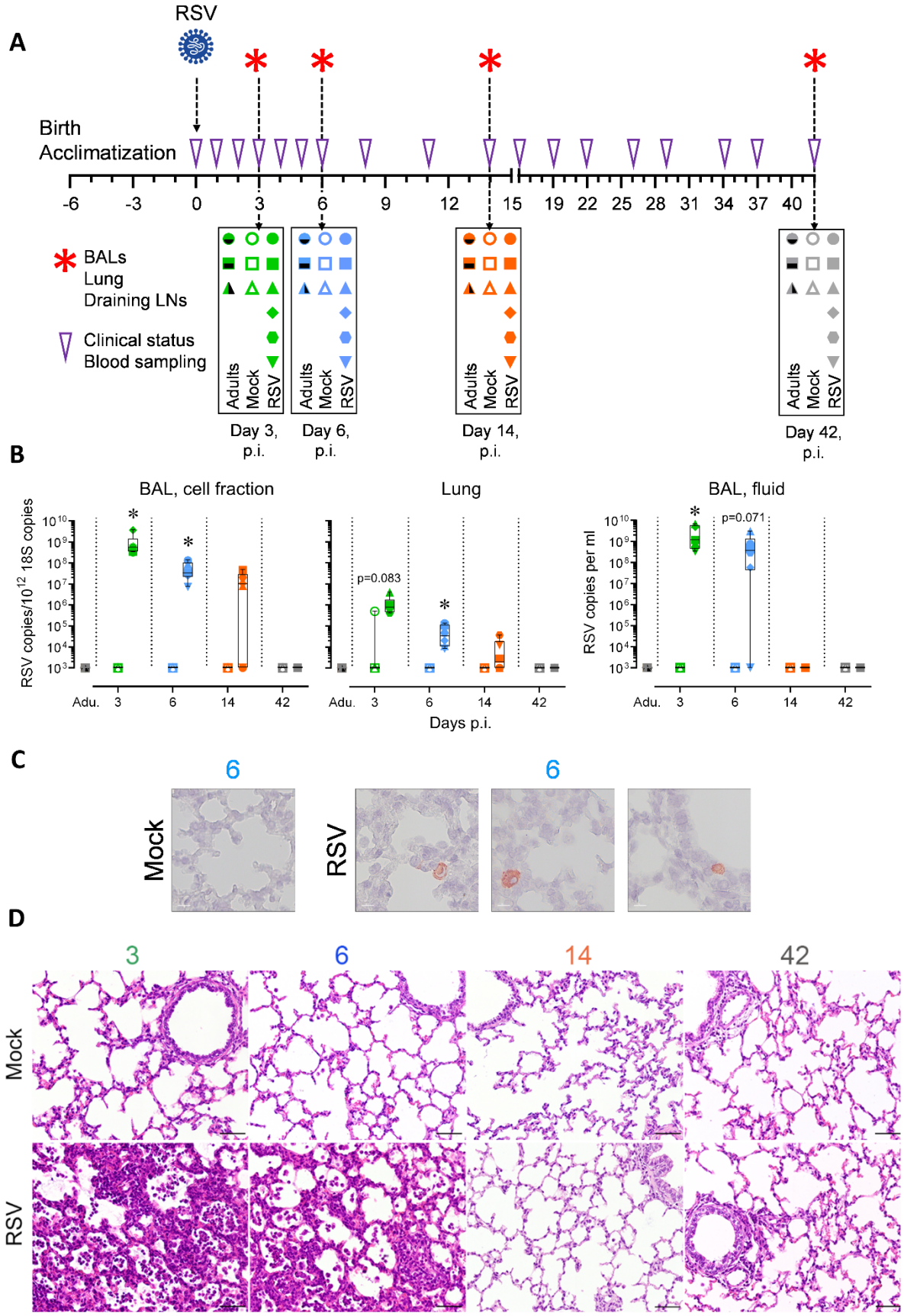

704

705 **Figure 2**

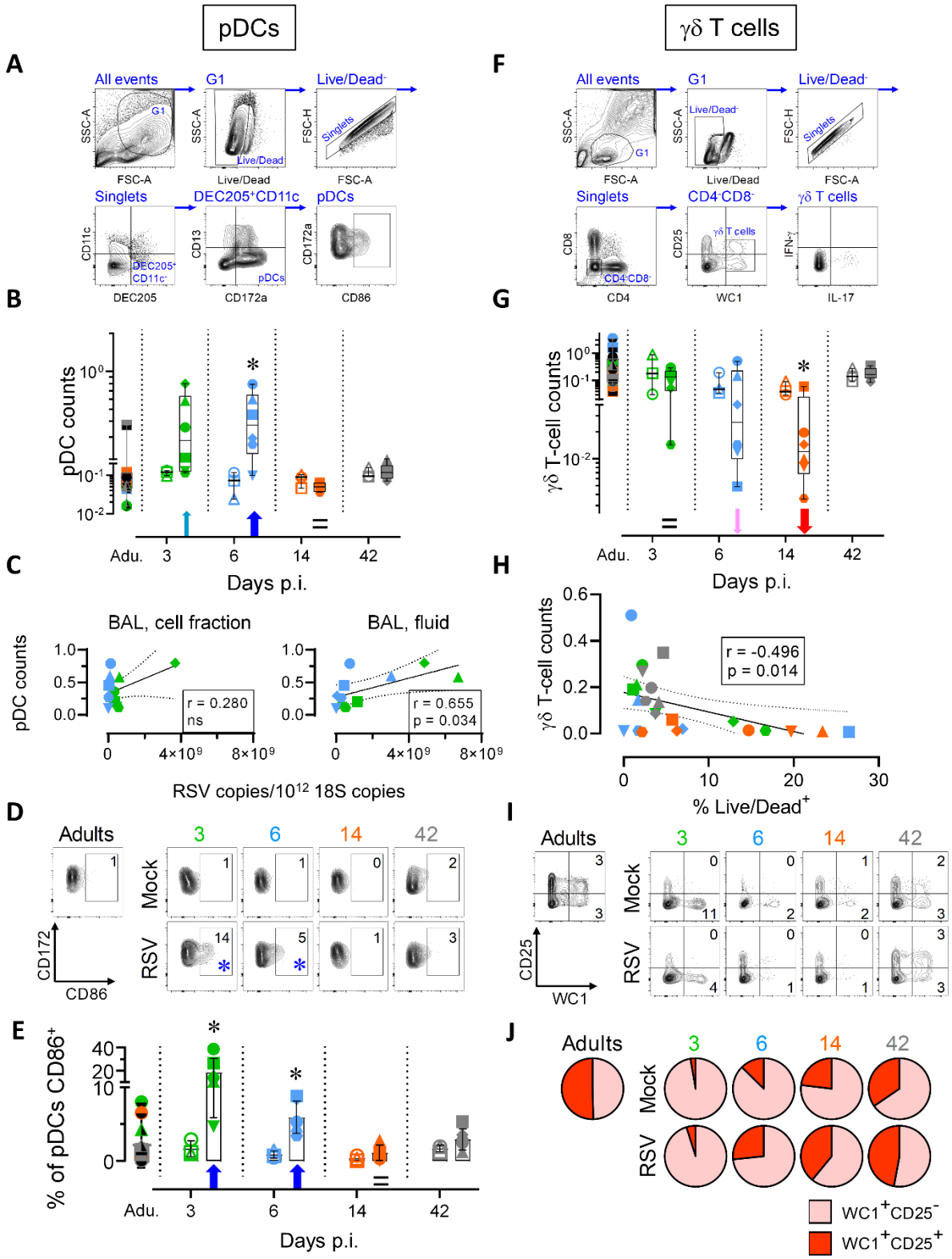

706

707 **Figure 3**

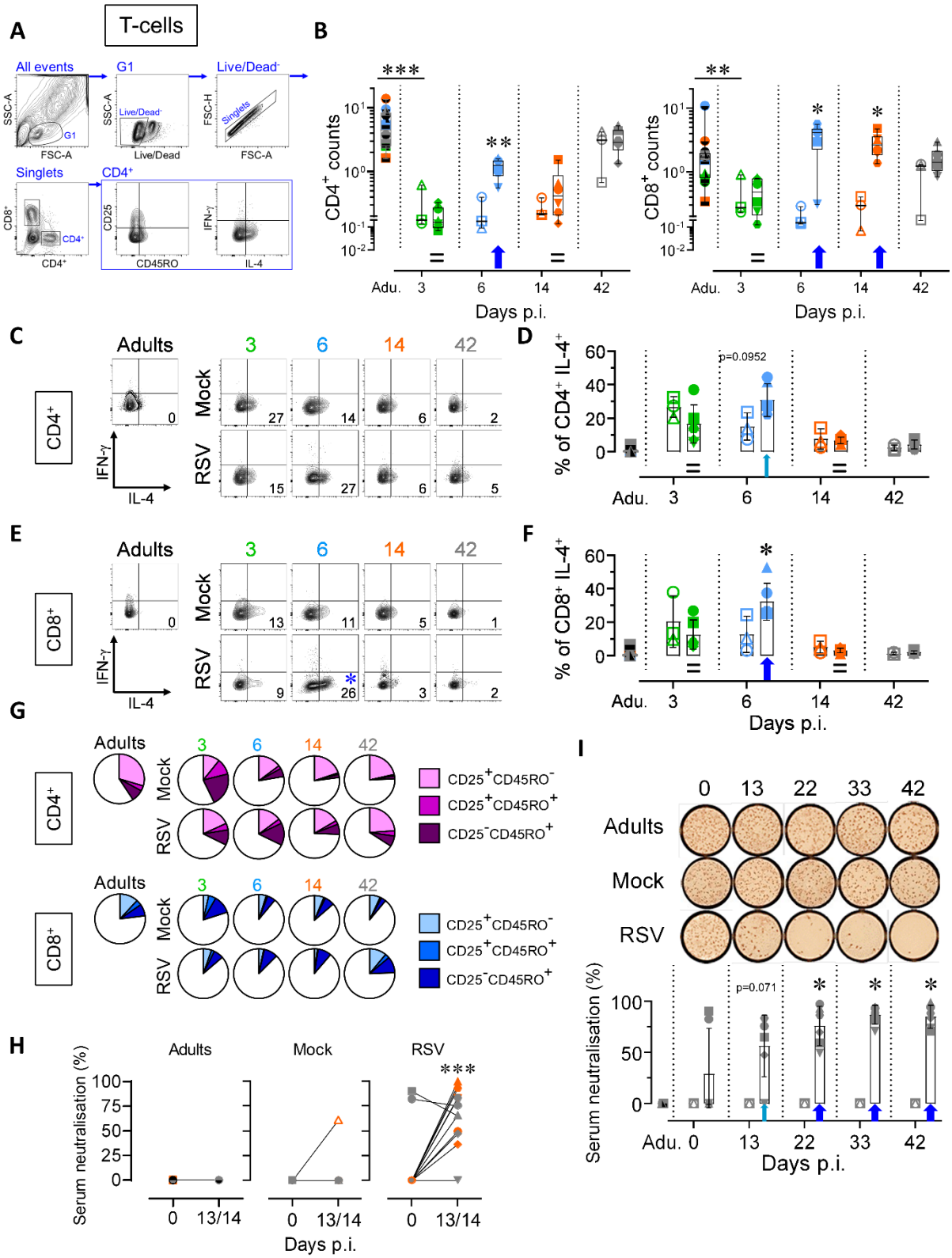

708

709 **Figure 4**

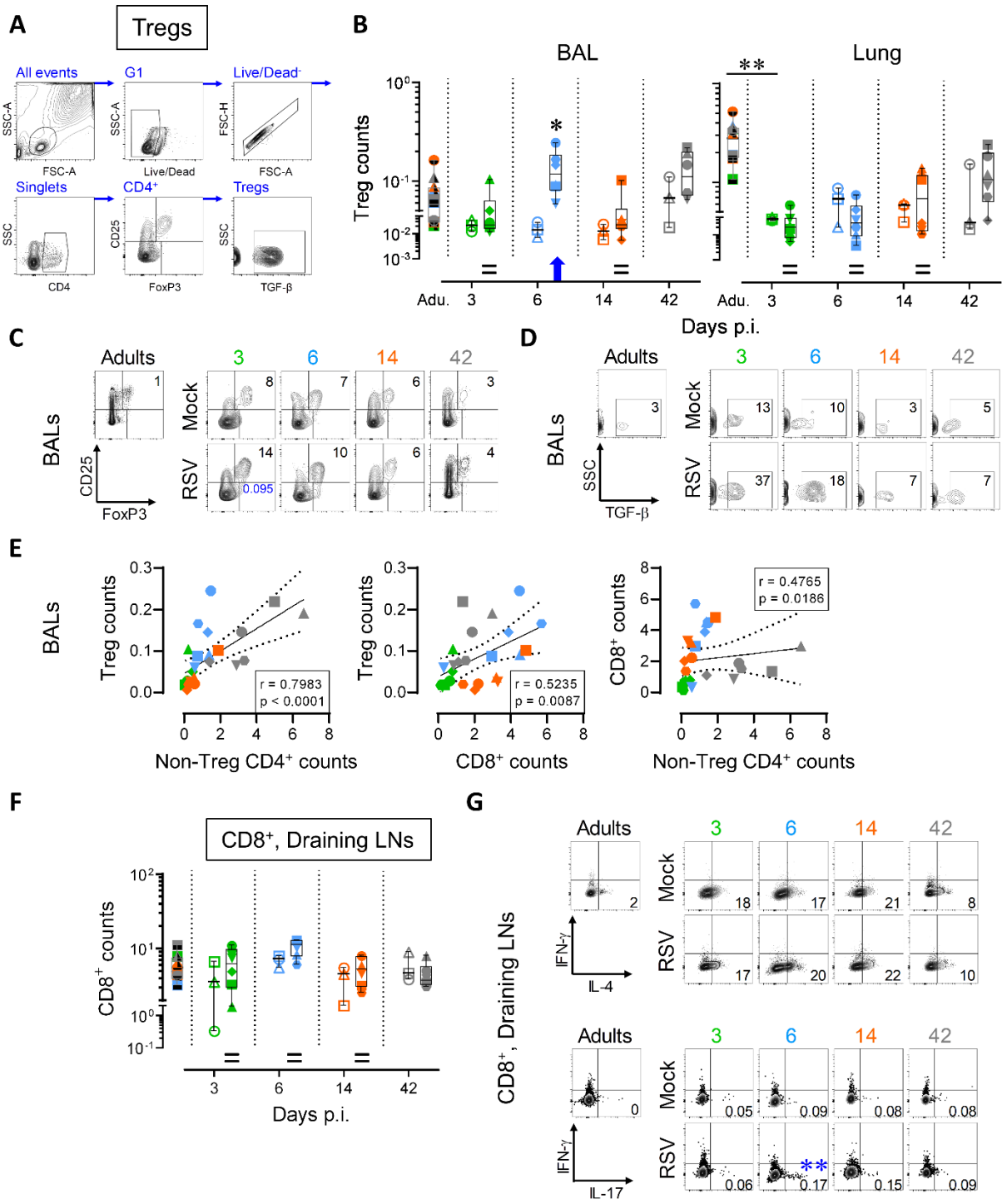

710

711 **Figure 5**

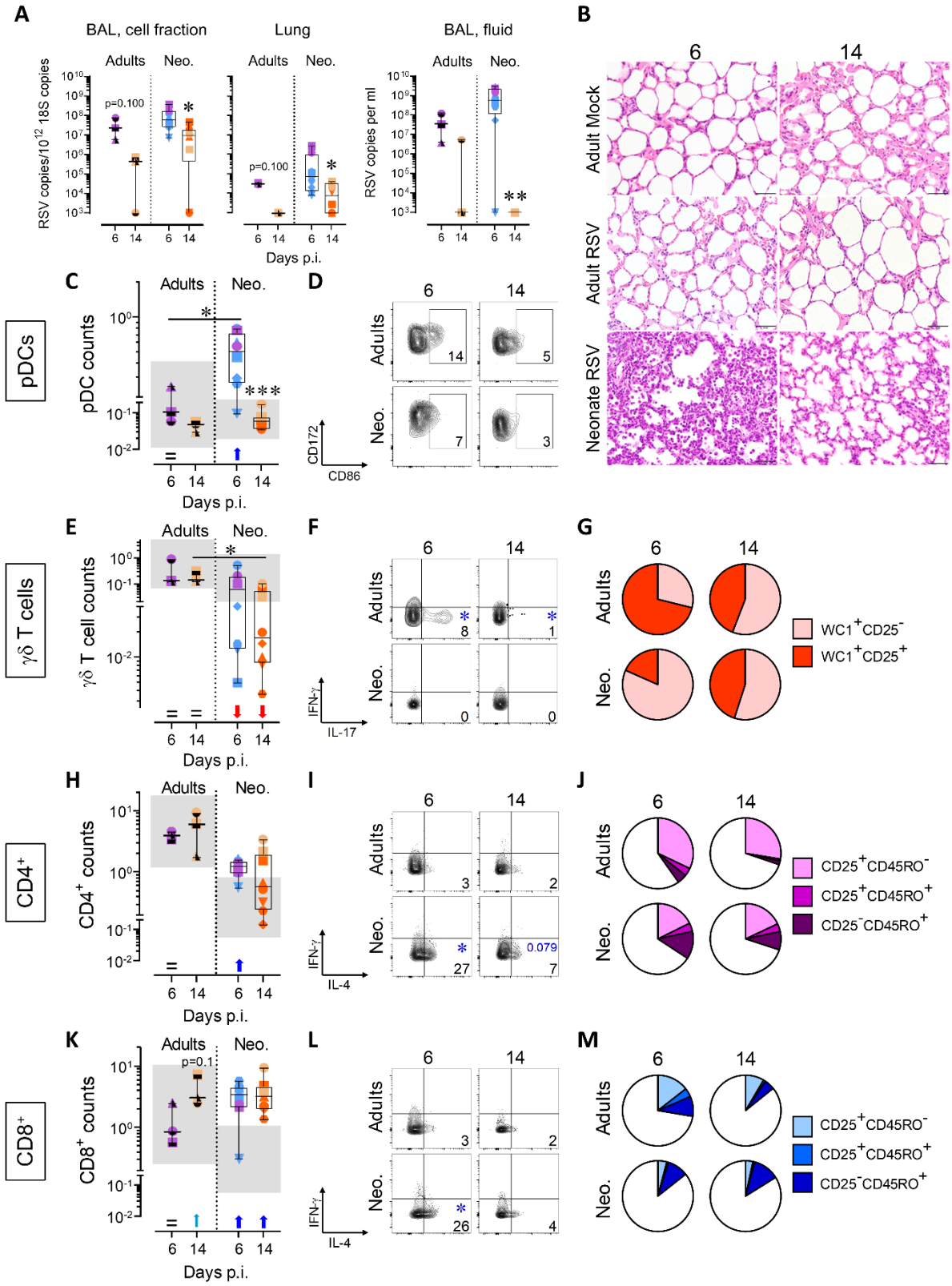

712

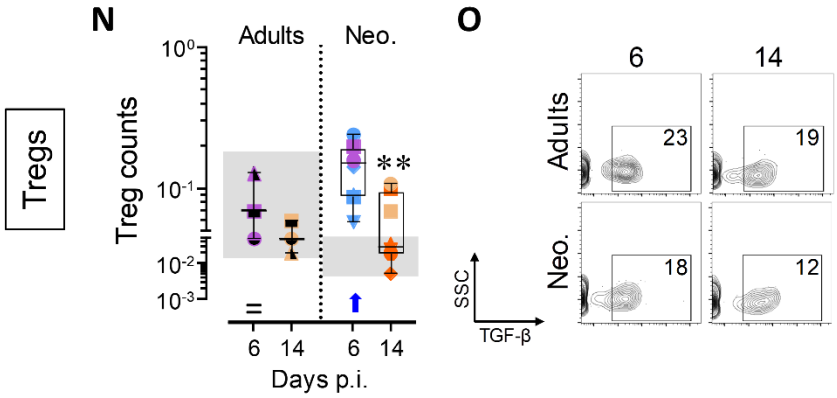
Tregs
N
Adults
Neo.
Treg counts
10^0
10^{-1}
10^{-2}
10^{-3}
=
**
6
14
6
14
Days p.i.
O
6
14
Adults
Neo.
23
19
18
12
SSC
TGF-β

713

714 **Figure 6**

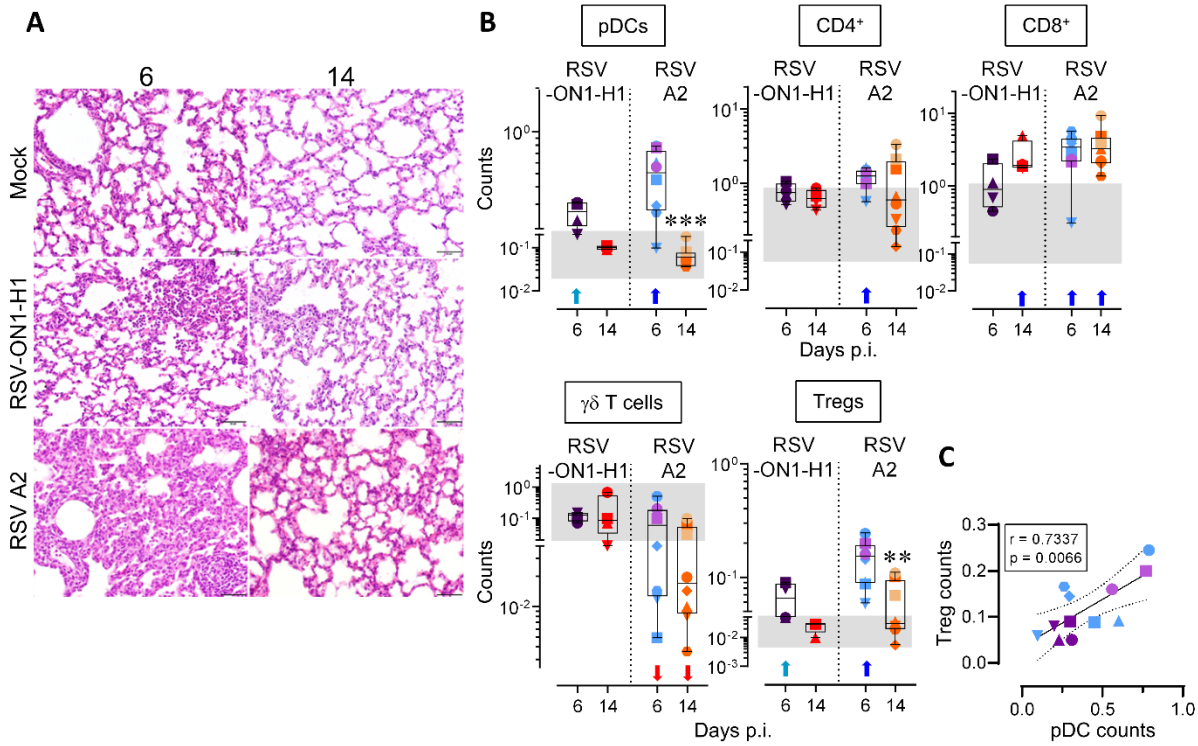

715